Technical Brief

On Residual Stresses in Arteries

C. J. Chuong[1] and Y. C. Fung[2]

Introduction

In the study of vascular elasticity the unloaded state (one with zero transmural pressure and zero axial load) is commonly used as the reference state in which stresses and strains are considered as zero everywhere. Strains at loaded states are defined with respect to this state. Stress-strain relationships are identified under the assumption that the vessel wall is stress-free at this unloaded state.

Evidence of the existence of residual stresses in the arterial wall at the unloaded state is given in Fung [4]. With a longitudinal cut along the vessel wall the unloaded specimen springs open and its cross section becomes a sector. The opening angle of the vessel wall is time-dependent after the sudden relief of the initial residual stress. It shows that the artery is not stress-free at the unloaded state.

It is important to identify the stress-free state. When we use pseudoelasticity [3] to characterize the arterial wall, we need a stress-free state as the reference state for strain measurements. Correspondingly, we also want to define stress with respect to this same reference state so that we can relate stresses to strains easily. Presence of the residual stress at the unloaded tube state will certainly affect the evaluation of stress distribution in the arterial wall due to actual loadings in the physiological range.

In this note we present a method to describe the geometry of the opened-up stress-free state of the artery, which is taken to be the reference state. An algorithm is outlined for the identification of the stress-strain relationship of the arterial wall. Residual stresses and strains in the unloaded tube are evaluated. With the consideration of residual stresses the stress distributions due to loadings in the physiological range are also evaluated.

Method

Geometric Description of the Stress-Free State. The artery is considered as a cylindrical tube whose wall material is homogeneous and cylindrically orthotropic [7]. Under this hypothesis, at the removal of residual stress from the unloaded state, the vessel wall should become a sector of constant curvature and thickness. Noncircular opened-up configuration similar to the photo of reference [4] are often obtained,

[1] Biomedical Engineering Program, University of Texas, Arlington, Tex. 76019
[2] Department of Applied Mechanics and Engineering Sciences/Bioengineering, University of California, San Diego, La Jolla, Calif. 92093

however. It can be due to adventitia tethering, experimental fixation handling difficulties, or other violations of the assumptions. In the following, a method is proposed to determine *the effective radii* and *the effective angle* for the stress-free reference state from the noncircular opened-up configuration taken from experiments.

Figure 1 shows the idealized vessel wall configurations at various states. We shall call the stress-free reference state as state 0, the unloaded state as state 1, and the subsequent loaded states as state 2, 3, . . N. With cylindrical polar coordinates, a material point is denoted as (R, Θ, Z) in the state 0 and (r, θ, z) in the states 1, 2, 3, . . N. The subscripts i and e indicate the internal and external wall radii at various states. Θ_o represents half of the angle of the arterial wall at the stress-free state 0.

The angle Θ_o and the internal and external wall radii for state 0 and state 1 can be determined from the direct measurements of fiber lengths at both surfaces taken from the photos of the open-up specimen. For state 1, it is obvious that

$$2\pi r_i = l_i, \qquad 2\pi r_e = l_e \qquad (1)$$

for the internal and external surfaces, respectively, where l denotes the measured fiber length. For state 0, we write

$$2\Theta_o R_i = L_i, \qquad 2\Theta_o R_e = L_e \qquad (2)$$

for the inner and outer walls where L denotes the fiber length measurements at this state. The determination of r_i and r_e for state 1 is straightforward. However, we need another equation to solve for the three unknowns, Θ_o, R_i, and R_e in equation (2). The incompressibility condition of the vessel wall [2] provides the third equation

$$\Theta_o (R_e^2 - R_i^2) = \pi \lambda_z (r_e^2 - r_i^2) \qquad (3)$$

where λ_z is the axial stretch ratio and is to be measured direct-

STATE 0   STATE 1   STATES 2,3...N

Pure Bending →

Pressurization / Axial Stretch →

(R, θ, Z) $\left[r^{(1)}, \theta^{(1)}, z^{(1)}\right]$ $\left[r^{(n)}, \theta^{(n)}, z^{(n)}\right]$
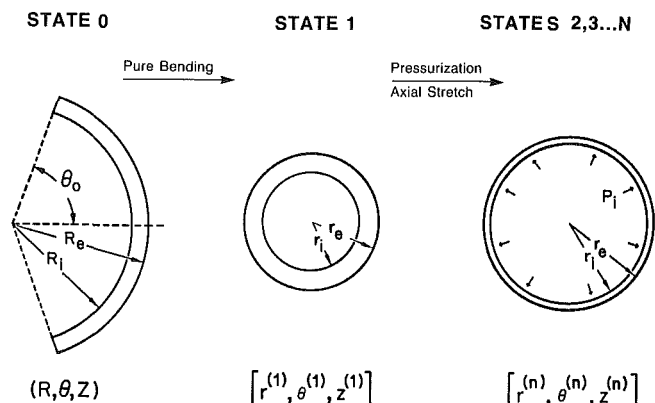
Fig. 1 The cross-sectional representation of an artery at the stress-free reference state 0, the unloaded tube state 1, and subsequent loaded states under transmural pressure and axial force

ly. By solving equations (2) and (3), the geometric description of state 0 is determined in terms of the effective values.

Identification of Material Constants. With the geometry of the reference state determined, the deformation of a thick-walled artery under transmural pressure and axial tethering can be described by the following expressions:

$$r = r(R), \quad \theta = (\pi/\Theta_o)\Theta, \quad z = z(Z) \tag{4}$$

for the transformation of the radial, circumferential, and longitudinal coordinates, respectively. The corresponding principal stretch ratios are

$$\lambda_r = \frac{\partial r}{\partial R}, \quad \lambda_\theta = \left(\frac{\pi}{\Theta_o}\right)\frac{r}{R}, \quad \lambda_z = \frac{\partial z}{\partial Z} \tag{5}$$

The arterial wall material is assumed to be characterized by a pseudo-strain energy function of the exponential type [3]

$$\rho_o W = \frac{c}{2} \exp(b_1 E_\theta^2 + b_2 E_z^2 + b_3 E_r^2 + 2b_4 E_\theta E_z$$
$$+ 2b_5 E_z E_r + 2b_6 E_r E_\theta) \tag{6}$$

where $\rho_o W$ represents the pseudo-strain energy per unit volume in the undeformed reference state. The constants c, b_1, b_2, b_3, b_4, b_5, b_6 characterize the wall material. E_θ, E_z, and E_r are Green's strains in the circumferential, longitudinal, and radial directions, respectively. They are related to the principal stretch ratios of equation (5) by

$$E_i = \frac{1}{2} (\lambda_i^2 - 1) \qquad (i = r, \theta, z) \tag{7}$$

The material is assumed to be incompressible. This constraint is added to the strain energy function through a Lagrangian multiplier. If X_α denotes the coordinates of a point at the reference state and x_i denotes that at the deformed state, then the Cauchy stress components can be obtained from

$$\sigma_{ij} = \frac{\rho}{\rho_o} \frac{\partial x_j}{\partial X_\alpha} \frac{\partial x_i}{\partial X_\beta} \frac{\partial}{\partial E_{\beta\alpha}} \rho_o W^* \quad (i,j,\alpha,\beta = r,\theta,z) \tag{8}$$

where ρ, ρ_o denote the densities of material in the deformed and undeformed states, respectively, and $\rho_o W^*$ is the modified strain energy function with incompressibility constraint.

The problem of a pre-strained thick-walled artery under transmural pressure and longitudinal tethering force can be solved by substituting equation (8) into the equation of equilibrium

$$\frac{\partial \sigma_r}{\partial r} + \frac{\sigma_r - \sigma_\theta}{r} = 0 \tag{9}$$

and the boundary conditions. The boundary conditions are that, 1) on the inner and outer surfaces $r = r_i$ and $r = r_e$, the vessel is subjected to pressures p_i and p_e, respectively; and 2) on the ends of the vessel segment, an external force F acts. Solving equation (9) with the use of two boundary conditions ($p_e = 0$), we obtain
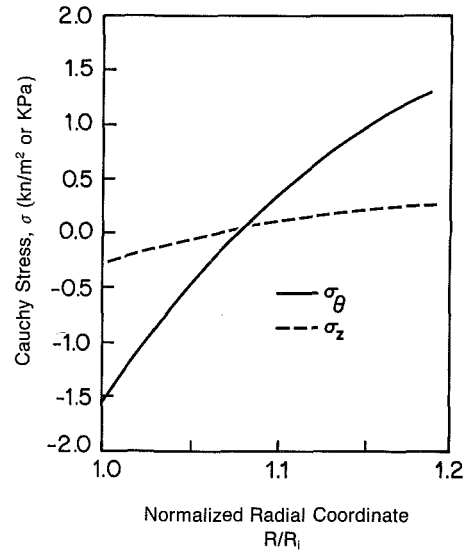
$$p_i = \int_{r_e}^{r_i} c\{(1 + 2E_r)[b_6 E_\theta + b_5 E_z + b_3 E_r]$$
$$- (1 + 2E_\theta)[b_1 E_\theta + b_4 E_z + b_6 E_r]\}e^Q \frac{dr}{r} \tag{10}$$

and

$$F = 2\pi c \int_{r_i}^{r_e} r e^Q [(1 + 2E_z)(b_4 E_\theta + b_2 E_z + b_5 E_r)$$
$$- \frac{1}{2} (1 + 2E_r)(b_6 E_\theta + b_5 E_z + b_3 E_r)$$
$$- \frac{1}{2} (1 + 2E_\theta)(b_1 E_\theta + b_4 E_z + b_6 E_r)]dr \tag{11}$$
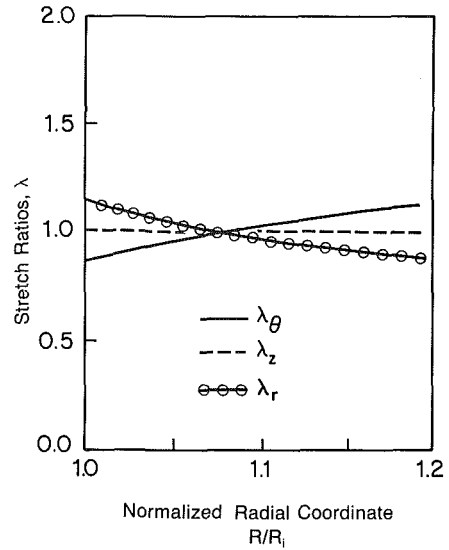
(a) Distributions of principal stretch ratios λ_θ, λ_z, λ_r

(b) Distributions of residual stresses σ_θ, σ_z

Fig. 2 Residual strain and stress in the wall of an unloaded rabbit thoracic artery

where Q denotes the exponent of equation (6).

Equations (10) and (11) are two integral equations from which we can determined the material constants. Once the material constants are determined, we can evaluate the residual stress at tube state 1 and the stress distribution at loaded states with residual stress taken into consideration.

Results

Geometric Description of the Reference State 0. To demonstrate the method in determining the geometry of the stress-free reference state, an example is given. From the data of reference [4] values of l_i, l_e, L_i, and L_e are measured to be 8.75, 12.5, 9.75, and 11.25 mm, respectively. Solving equations (2) and (3), with the assumption of $\lambda_z = 1$, we obtain $R_e = 4.52$ mm, $R_i = 3.92$ mm, and $\Theta_o = 71.4$ deg as *the effective external, internal radii* and *the effective angle* for the reference state 0.

Residual Strain and Stress at State 1 (Tube Unloaded). Figure 2(a) shows the residual strain in the arterial wall

when the vessel is unloaded. The strains are expressed in terms of principal stretch ratios. It is seen that fibers at the inner wall are shortened, while those at the outer wall are elongated. The location of neutral surface can be obtained from the second of equation (5) by setting $\lambda_\theta = 1$, yielding in this example a location at 43 percent of the wall thickness measured from the internal surface.

To illustrate the method of calculating the residual stress at the unloaded state and the stress distribution at the loaded states, we shall use the raw data of Exp:71 on rabbit thoracic artery from Fung et al. [5]. It is assumed that the residual strain in the artery of Exp:71 is distributed like that of the artery in reference [4]. We then solved equations (10) and (11) for material constants to obtain $c = 22.40$ kPa, $b_1 = 1.0672$, $b_2 = 0.4775$, $b_3 = 0.0499$, $b_4 = 0.0903$, $b_5 = 0.0585$, $b_6 = 0.0042$. We then used these constants to evaluate the stresses at various states of loading. Figure 2(b) shows the distribution of the residual stresses at the unloaded state. In the circumferen-
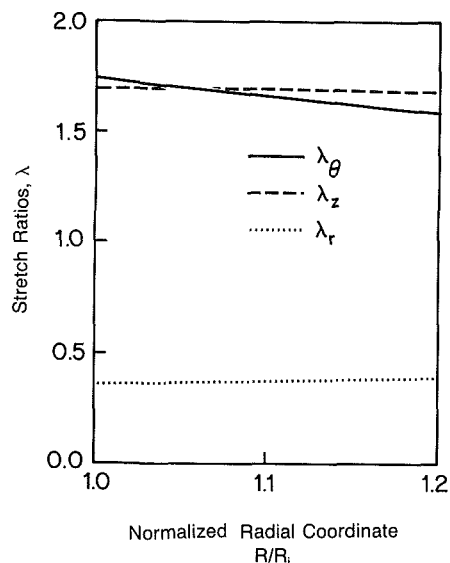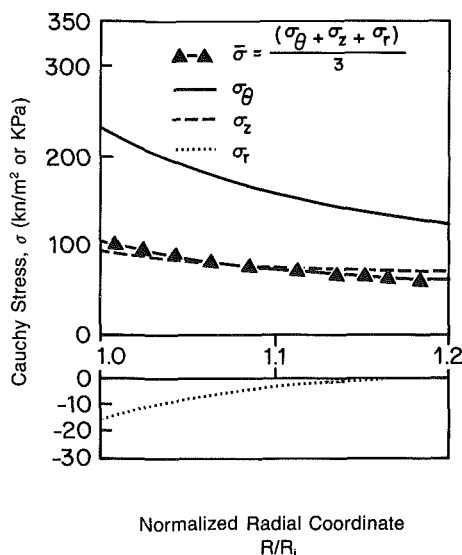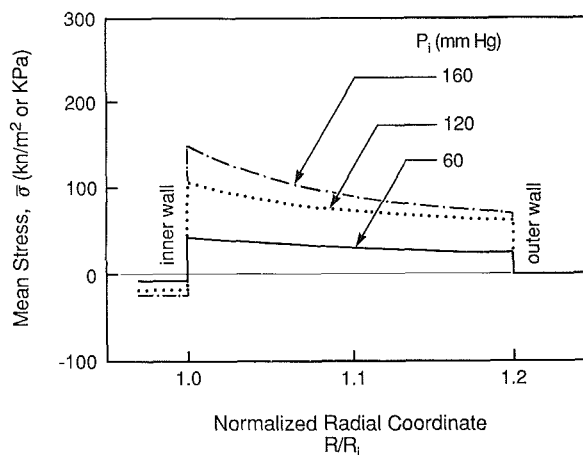

Fig. 4 The mean dilatational stress distribution in the vessel wall is plotted for three transmural pressures, p_i = 60, 120, 160 mmHg with p_e = 0 mmHg. Note the large jump from the pressure in the lumen p_i to the mean stress at the inner wall.

tial direction, the inner wall has a compressive residual stress of 1.5 kPa; the outer wall has a tensile residual stress of 1.3 kPa. These are small numbers compared with stresses at loaded states shown in Fig. 3, but their effects are large, as will be shown in the forthcoming. At this unloaded state the vessel wall is in a state of pure bending.

Strain and Stress Distributions at Loaded States. Figures 3(a) and (b) show the distributions of principal stretch ratios and principal stresses of the vessel wall at $p_i = 120$ mmHg (16 kPa) and axial stretch ratio = 1.691. The circumferential stress at the inner wall is found to be 1.42 times larger than the average value across the vessel wall. In a previous work [1], under the hypothesis that the unloaded tube is stress-free, we obtained that: at $p_i = 120$ mmHg, the circumferential stress at the inner wall was 6.5 times larger than the average value across the vessel wall. Hence the removal of the hypothesis that the unloaded state is stress-free has the effect of reducing the stress concentration factor from 6.5 to 1.42. In the present work, we identified the stress-free state from experimental results, evaluated the residual strain and stress at the unloaded tube state, and calculated the strain and stress at various internal pressures. Compared with our former work [1], the results in Fig. 3 show that the residual stress in the unloaded tube state, although small in magnitude, is significant in reducing the high stress concentration.

The distribution of the mean dilatational stress across the vessel wall is shown in Fig. 4 for $p_i = 60, 120, 160$ mmHg. At 60 mmHg, the mean stress is rather uniform across the wall thickness. At 120 mmHg, it is 105 kPa at the inner wall and 60 kPa at the outer wall. At 160 mmHg, it becomes 140 kPa at the inner wall and 75 kPa at the outer wall. This suggests that, as the pressure varies from 60 to 160 mmHg, the driving force for fluid movement in the arterial wall can change significantly at the inner layer. The mean dilatational stress is the negative of hydrostatic pressure, which is considered as the driving force for fluid movement in the arterial wall. Note the large jump in the mean stress (from p_i to $\bar{\sigma}$) at the inner and outer walls of the vessel. Fluid movement from the lumen into the arterial wall is due largely to these jumps. The literature on this subject and the interpretation of its relationship to atherogenesis is discussed in reference [1].

(a) Distributions of principal stretch ratios λ_θ, λ_z, λ_r

(b) Distributions of Cauchy stresses σ_θ, σ_z, σ_r and the mean stresses $\bar{\sigma}$

Fig. 3 Strain and stress distributions in the wall of a rabbit thoracic artery at p_i = 120 mmHg (~16.0 kPa) and λ_z = 1.691

References

1 Chuong, C. J., and Fung, Y. C., 1983, "Three-Dimensional Stress Distribution in Arteries," ASME JOURNAL OF BIOMECHANICAL ENGINEERING, Vol. 105, pp. 268–274.

2 Chuong, C. J., and Fung, Y. C., 1984, "Compressibility and Constitutive Equation of Arterial Wall in Radial Compression Experiments," *Journal of Biomechanics*, Vol. 17, pp. 35-40.

3 Fung, Y. C., 1981, *Biomechanics: Mechanical Properties of Living Tissues*, Springer-Verlag, New York.

4 Fung, Y. C., 1984, *Biodynamics: Circulation*, Springer-Verlag, New York, pp. 59-60.

5 Fung, Y. C., Fronek, K., and Patitucci, P., 1979, "Pseudoelasticity of Arteries and the Choice of its Mathematical Expression," *American Journal of Physiology*, Vol. 237, pp. H620-H631.

6 Green, A. E., and Adkins, J. E., *Large Elastic Deformations*, 2nd Edition, Clarendon Press, Oxford, 1970.

7 Patel, D. J., and Fry, D. L., 1969, "The Elastic Symmetry of Arterial Segments in Dogs," *Circulation Research*, Vol. 24, pp. 1-8.

8 Patitucci, P., "Computer Program for Fitting Pseudo-Strain Energy Functions to Soft Tissue Experimental Stress and Strain Data," Digital Equipment Users Society, DECUS, No. 11-548, One Iron Way, Malboro, Mass., 1982.